Peer-reviewed version available at *Chinese Journal of Polymer Science* **2019**, *37*; doi:10.1007/s10118-019-2195-2

Positron spectroscopy of polyvinylidene fluoride after helium ions irradiation

Roman Laptev, Lyu Jinzhe, Natalya Dubrova

(Division for Experimental Physics, School of Nuclear Science & Engineering, National Research Tomsk Polytechnic University, Lenina Ave. 43, Tomsk, 634034 Russia,)

laptevrs@tpu.ru

*corresponding author 2891796456@qq.com

dubrova@tpu.ru

ABSTRACT

Free volume is an extremely important intrinsic defect in polymers. Structurally, the free volume is the randomly distributed holes in the polymer molecular chain segments. From the perspective of molecular movement, it is also the space needed for the movement of molecular segments. In proton exchange membrane fuel cells, the free volume is also the space needed for the directional conduction of protons. Irradiation grafting sulfonated polyvinylidene fluoride (PVDF) is one of the methods to produce proton exchange membrane with good proton channel rate. Using the LYS-1 program, based on the linear absorption coefficient and backscatter coefficient models, the percentage of annihilated positrons in PVDF in the two-layer model and the three-layer model was studied, and comparing the two fitting results it is determined that the model closest to the positron annihilation percentage required by the PALS experiment is the two-layer model, which allows the percentage of positrons that are annihilated in PVDF films with a thickness of 100 μm to reach 46% using the high energy positron source ^{44}Ti without using the positron moderator. Using positron annihilation lifetime spectrum (PALS) analysis methods, based on Eldrup's classical model of free volume, the influence of absorbed doses of α particles on the free volume and crystallinity of PVDF was investigated, respectively. Based on the two test results the model of cross-linking and degradation of polyvinylidene fluoride irradiated by α particles was determined. Afterwards, X-ray diffraction (XRD) methods was used to study the change of PVDF crystal area before and after irradiation. The XRD results are consistent with the results measured by PALS.

Keywords: positron annihilation, free volume, crystallinity, XRD, polyvinylidene fluoride, helium ions, absorbed dose, cross-linking, degradation, Braking ability, linear absorption coefficient, Backscatter coefficient, bremsstrahlung

1. Introduction

The research and application of irradiation effects on polymers have been paid more and more attention. The chemical changes of polymers caused by absorbed doses is not large. However, the induced changes of physical and mechanical properties of polymers are significant. Regardless of cross-linked or degradable polymers, their inherent physical, chemical, and mechanical properties can be severely damaged when the absorbed dose is high to a certain degree, which causes materials to be unusable [1-4]. Therefore, radiation stability or radiation resistance is one of the important properties of polymers, especially when polymers are used in the nuclear reactor or aerospace industry. PALS is the only sensitive method for studying the microstructure of amorphous polymers – the parameter of free volume with atomic size [5-8]. Using the method of PALS, it was found that the influence of radiation on polymers is related to both the type of radiation and the type of polymers, as well as the irradiation power. For example, M. S. Abd El Keriem [9] investigated effect of Low Gamma-Irradiated dose on the structure of cellulose triacetate Films and found that I_3 shows an increase from 0 to 10 kGy. Such an increase of I_3 is mainly due to the presence of carbonyl groups, which are formed during irradiation [10]. With a further increase in the dose to 15 kGy, I_3 shows a gradual decrease, and then approaches a constant to 25 kGy, which is well known for γ-irradiated polymers [11]. Such behavior may indicate that stability in the structure has been achieved. Xianyi ZHOU [12] and his collaborators obtained results on the change of free volumes in γ- irradiated polytetrafluoroethylene (PTFE) and polyethylene. It is found that from 0 to 300 kGy the crystallinity of PTFE continuously increases and the size of the free volume gradually decreases, while in polyethylenes both parameters show the opposite behavior depending on the dose. Khalid S. Jassim and his collaborators [13] investigated the properties of free volumes in beta-irradiated high density polyethylene (HDPE). It is indicated that both free volumes and I_3 increase at a dose less than 1.5 Gy, followed by a decrease to a constant volume at a dose of 1.5 to 12 Gy. These studies indicate that many factors influence the characteristics of the interaction of radiation with substances, one of which is the radiation resistance of polymers. Possessing high resistance to different types of radiation, polymers show a structural change only at a high radiation dose (several hundred kGy), otherwise the polymer structure changes and approaches a stable state even at a sufficiently low radiation dose (several Gy).

Positron annihilation technique is one of sensitive tools for investigating microscopic defects and phase transition of materials. In normal positron spectroscopy, the positron energy is in the order of MeV and the depth of injection in the sample is deep for the research of average defect density in the material. In order to achieve this goal, it is usually required that the amount of

annihilation positrons in the sample be no less than 50% of the amount of positrons emitted from the positron source This places stringent requirements on the positron source and the thickness of sample. The positron emitted by ^{22}Na has a maximum energy of 0.545 MeV, the injection depth of which in metal is usually 0.3 to 1 mm, and is 1 to 2 mm in a polymer material with a small density [14]. ^{44}Ti is a high-energy positron source that produces positrons with a maximum energy of 1.47 MeV, the injection depth of which will be greater in the polymer material compared to positrons emitted by ^{22}Na. PVDF is a material used to prepare modified proton exchange membranes [15, 16, 17]. Due to its working environment, it is required to have a thickness in the range of 20-100 μm (a greater ohmic overpotential will be generated if it exceeds this range) [18, 19, 20]. Since the positron energy produced by ^{44}Ti is in the order of MeV, and the thickness of PVDF is very small, only a few positrons are annihilated in PVDF, and most of the positrons penetrate the film without annihilation. In order to annihilate 50% of positrons in PVDF and not to use positron moderators for cost savings, this paper proposes a method to make the annihilated positron percentage in PVDF close to 50%, which is in good agreement with the requirements of the PALS method.

In this paper, PALS and XRD are combined with free volume theory to study the influence of helium ions irradiation on the microstructure of PVDF, so as to reveal the relationship between the microstructure changes and absorbed dose.

2. Development of a model for increasing the number of annihilation positrons in the sample layer PVDF

The transfer profile or the path of positrons through the material is calculated using the LYS-1 program, which is based on a multi-scattered model [21, 22]. For the calculation, only the linear absorption coefficient, backscatter factor and material thickness are required.

Linear absorption coefficient is [23]:

$$\alpha_+ = \frac{12.6Z^{0,17}\rho}{E_{max}^{1,28}}, \quad (1)$$

where

z – the atomic amount of the substance;

E_{max} – maximum positron energy, Mev;

ρ – the density of the substance, g.

Backscatter coefficient is [24]:

$$R = 0.42 \log_{10} Z - 0.146, \quad (2)$$

In positron annihilation measurements, in order to ensure that all positrons are annihilated in the measured material, the sample and the radioactive source must adopt a "sandwich" structure, that is, the same sample is placed on both sides of the source. In addition, in order to make a great amount of incident positrons stay in the material, an ordinary method is making the thickness of the sample be greater than the incident depth of positrons. For PVDF polymers with small thickness to increase the amount of annihilated positrons in films, the following two models are developed, while the positron source is ^{44}Ti, which emits positrons with a maximum energy of 1.47 MeV:

1) two-layer model: source e^+ + PVDF (first layer) + metal (second layer) (fig.1).

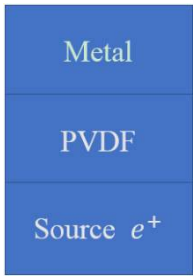

Fig.1. One side of "sandwich" structure of two-layer model: source e^+ + PVDF (first layer) + metal (second layer).

2) three-layer model: source e^++ polymer (first layer) + PVDF (second layer) + Pb (third layer) (fig. 2)

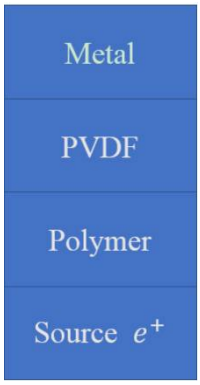

Fig.2. One side of "sandwich" structure of three-layer model: source e^++ polymer (first layer) + PVDF (second layer) + Pb (third layer)

According to the formulas (1), (2), in order to obtain the linear absorption coefficient and backscatter coefficient of each layer, it is necessary to know the energy of positrons that reach to

the surface of each layer. This requires that the energy loss of positrons in each layer must be known, which is determined by braking ability of each layer for positrons.

The energy loss of positrons in substance is divided into two types: the collision loss and bremsstrahlung energy losses. The collision loss of positron energy is determined by the following formula:

$$(-\frac{\mathrm{d}E}{\mathrm{d}x})_{col} = \frac{2\pi {r_e}^2 m_e c^2}{\beta^2} N_A \frac{Z_2}{A} \times \left[2\ln(\frac{\beta^2}{1-\beta^2}\frac{\varepsilon}{2(I^*/m_e c^2)^2}\right) + F^+(\varepsilon)], \quad (3)$$

Where

Z_2 – the atomic amount of the substance;

r_e – the classical radius of an electron, cm;

m_e – mass of an electron, g;

N_A – constant avogadro;

a – atomic mass of substance, a.e.m;

c – speed of light, cm/s;

I^* – the average excitation energy of the substance's atom, erg;

v – positron velocity, cm/s;

$\beta = \frac{v}{c}$;

$\varepsilon = \frac{T}{m_e c^2}$;

T – kinetic energy of a positron, эрг;

$F^+(\varepsilon)$ – function for positrons;

$$F^+(\varepsilon) = 2\ln 2 - \frac{\beta^2}{12}[23 + \frac{14}{\varepsilon+2} + \frac{10}{(\varepsilon+2)^2} + \frac{4}{(\varepsilon+2)^3}], \quad (4)$$

The bremsstrahlung energy losses of positrons related to the bremsstrahlung energy losses of electronics. In the Born approximation without taking shielding into account, the calculation of the braking ability caused by the radiation of electrons with non-relativistic energies gives the following result:

$$(-\frac{\mathrm{d}E}{\mathrm{d}x})_{rad} = \frac{16}{3} 3.44 \cdot 10^{-4} \frac{Z_2(Z_2+1)}{\mathrm{A}} T_0, \quad (5)$$

Where

T_0 - kinetic energy of electrons, MeV;

A – atomic mass of substance, a.e.m;

For the relativistic case:

Preprints (www.preprints.org) | NOT PEER-REVIEWED | Posted: 3 September 2018 doi:10.20944/preprints201809.0019.v1

Peer-reviewed version available at Chinese Journal of Polymer Science 2019, 37; doi:10.1007/s10118-019-2195-2

$$(-\frac{\mathrm{d}E}{\mathrm{d}x})_{rad} = 3.44 \cdot 10^{-4} \frac{Z_2(Z_2+1)}{A} T_0 \, (4 \ln \frac{T_0}{0.255} - \frac{16}{3}), \quad (6)$$

The loss of positron energy to radiation can be calculated by loss of electrons, multiplying them by the function:

$$\eta(\frac{T_0}{{Z_2}^2}) = \begin{cases} 0, x \le -8 \\ \frac{1}{2} + \frac{1}{\pi} \mathrm{arctg}(0.415x + 0.0021x^3 + 0.00054x^5), -8 < x < 9, \\ 1, \ x \ge 9 \end{cases} \quad (7)$$

Where $x = \ln(7.52 \cdot 10^6 \frac{T_0}{{Z_2}^2})$, T_0 в GeV.

The total energy losses of positrons on per unit path (total braking ability) are equal to the sum of energy losses due to collisions and radiation [25]

$$-\frac{\mathrm{d}E}{\mathrm{d}x} = (-\frac{\mathrm{d}E}{\mathrm{d}x})_{col} + (-\frac{\mathrm{d}E}{\mathrm{d}x})_{rad}, \quad (8)$$

Table 1 shows the amount of annihilated positrons in PVDF using different metals as the material of the second layer**.**

Table 1. – Results of calculation for the **two-layer** model "source e^+ + PVDF (first layer 20 μm) + metal (second layer)."

Metal name	Linear absorption coefficient,	Backscatter coefficient	The amount of annihilated positrons in the first layer, %
Al	33	0.23	20.40
Fe	107	0.34	23.00
Ni	123	0.35	23.28
Cu	124	0.35	23.28
Zn	100	0.36	23.56
Zr	95	0.4	24.74
Nb	126	0.41	25.06
Sn	111	0.44	26.04
Pb	188	0.51	28.70

It can be seen from Table 1 that in the two-layer model the maximum amount of annihilated positrons in PVDF was obtained using Pb as the material of the second layer, which has the largest backscattering coefficient of all the metals listed.

Since the location of the Pb metal behind the PVDF film allows the most significant increase in the amount of annihilated positrons in a PVDF film, it is necessary to settle calculation for the

Preprints (www.preprints.org) | NOT PEER-REVIEWED | Posted: 3 September 2018 doi:10.20944/preprints201809.0019.v1

Peer-reviewed version available at Chinese Journal of Polymer Science 2019, 37; doi:10.1007/s10118-019-2195-2

model "source e^++ PVDF (first layer) + Pb (second layer)" with different thicknesses of the PVDF film (Table 2).

Table 2. – Results of calculation for the model "source e^++ PVDF (first layer) + Pb (second layer)":

PVDF thickness, μm	The amount of annihilated positrons in a PVDF film,%
50	28.70
70	36.90
100	46.94

In this model, a polymer is placed on layer 1 in order to hold back the positrons. Three different polymers are taken for calculation: polyethylene C_2H_4 (PE), PVDF $C_2H_2F_4$ and Teflon (PTFE)(C_2F_4). Table 3 and Table 4 show the amount of annihilated positrons in PVDF using C_2H_4, $C_2H_2F_4$ and C_2F_4 as the material of the first layer with various thicknesses.

Table 3. – Results of calculation for the **tree-layer** model "source e^+ + polymer (first layer) + PVDF (second layer) + Pb (third layer)" with a thickness of the second layer of 50 μm:

Name of polymer	Thickness of the first layer, μm	Braking capacity of the first layer, MeV/μm	The energy of the positrons falling to the second layer E_2, MeV	The amount of annihilated positrons in the second layer,%
Polyethylene (C_2H_4)	50	$2.76*10^{-4}$	1.46	24.60
	70	$2.76*10^{-4}$	1.45	24.44
	100	$2.76*10^{-4}$	1.44	23.30
PVDF ($C_2H_2F_2$)	50	$3.88*10^{-4}$	1.45	22.24
	70	$3.88*10^{-4}$	1.44	20.10
	100	$3.88*10^{-4}$	1.43	17.92
Polytetrafluoroethylene (PTFE) (C_2F_4)	50	$3.41*10^{-4}$	1.45	19.46
	70	$3.41*10^{-4}$	1.45	17.80
	100	$3.41*10^{-4}$	1.44	17.70

Preprints (www.preprints.org) | NOT PEER-REVIEWED | Posted: 3 September 2018 doi:10.20944/preprints201809.0019.v1

Peer-reviewed version available at Chinese Journal of Polymer Science 2019, 37; doi:10.1007/s10118-019-2195-2

Table 4. – Results of calculation for the **tree-layer** model "source e^+ + polymer (first layer) + PVDF (second layer) + Pb (third layer)" with the thickness of the second layer of 100 μm:

Name of polymer	Thickness of the first layer, μm	Braking capacity of the first layer, MeV/μm	The energy of the positrons falling to the second layer is E_2, MeV	The amount of annihilated positrons in the second layer, %
Polyethylene (C_2H_4)	50	$2.76*10^{-4}$	1.46	40.80
	70	$2.76*10^{-4}$	1.45	40.40
	100	$2.76*10^{-4}$	1.44	37.80
PVDF ($C_2H_2F_2$)	50	$3.88*10^{-4}$	1.45	37.00
	70	$3.88*10^{-4}$	1.44	33.68
	100	$3.88*10^{-4}$	1.43	29.36
Polytetrafluoroethylene (PTFE) (C_2F_4)	50	$3.41*10^{-4}$	1.45	32.74
	70	$3.41*10^{-4}$	1.45	29.96
	100	$3.41*10^{-4}$	1.44	24.98

From the data shown in Tables 3, 4, it follows that the larger the proportion of hydrogen atoms in the polymer (first layer), the smaller the thickness of the polymer (first layer), the larger the thickness of PVDF (second layer), the larger the amount of annihilated positrons in PVDF (second layer).

In order to increase the amount of annihilated positrons in a PVDF film, two models were developed, differing from one another in the amount of layers.

The first model is the two-layer model. In this model, the maximum amount of positrons annihilated in the PVDF film was obtained using lead (Pb) as the material of the second layer, which has the greatest backscatter coefficient from all the metals considered in the work. With a thickness of PVDF film 100 μm, the amount of annihilated positrons is 46.94%

The second model is the three-layer model. The essence of this model is that any material should be placed on the first layer in order to reduce positron energy.

In comparison with the three-layer model, the two-layer model allows obtaining a larger amount of annihilated positrons in a PVDF film. The disadvantages of the three-layer model include the following:

1) The braking ability of polymers (the first layer) is in the range $(1\sim4)\cdot10^{-4}$ MeV/μm, then the energy losses of the positrons in the first layer are:

$$\Delta E = \frac{dE}{dx}\cdot h_1 \leq (4\cdot10^{-4}\ \text{MeV/μm})\cdot(100\ \text{μm}) = 0.04\ \text{MeV}$$

The energy of the positrons emitted from the source ^{44}Ti:

$$E_1 = 1.47 \text{ MeV}$$

The energy of positrons incident on the second layer (PVDF film):

$$E_2 = E_1 - \Delta E \geq 1.47 \text{ MeV} - 0.04 \text{ MeV} = 1.43 \text{ MeV}$$

It is observed that polymer materials almost can't reduce the energy of positrons. When the thickness of the second layer (PVDF) is increased to 100 μm, the maximum amount of annihilation positrons in the PVDF film is only 40.80%.

2) As already mentioned above, the smaller the thickness of the polymer (first layer), the greater the amount of annihilated positrons in the PVDF film (the second layer), i.e. with a polymer thickness of zero, the maximum amount of annihilated positrons in a PVDF film (the second layer) is observed, and this is a two-layer model.

3. Experimental set-up

3.1. Sample preparation and irradiation

The sample under investigation is F-2M (PVDF) films with a thickness of 20 μm produced by "Fluoropolymer" (St. Petersburg). The R-7M accelerator of physicotechnical institute of Tomsk Polytechnic University was used as a source of ionizing radiation producing a beam of helium ions with energy 27 MeV discharged into the air. Absorbed dose rate is 0.26 MGy/min, total absorbed doses are 0.13, 0.26, 0.395, 0.525, 0.655 MGy respectively. The corresponding sample code is PVDF0, PVDF0.5, PVDF1, PVDF1.5, PVDF2, PVDF2.5.

3.2. PALS Analysis

A conventional fast–fast coincidence spectrometer with a time resolution 240 ps was used for PALS measurements [26, 27]. In PALS spectrum about 3-5 million counts were accumulated. The PALS spectra were analyzed into three components (τ_1, τ_2 and τ_3) with their intensities (I_1, I_2 and I_3) using MELT. At present, several computer programs with various mathematical models have been developed to obtain the spectrum of PALS. PATFIT-88 [28], considering the spectrum of the PALS as a convolution of superposition of multiexponential components with the instrument's resolution function, estimates the parameter values based on the method of semi-linear least squares; LifeTime10 [29] obtains the PALS spectrum the same as PATFIT-88, but estimates the parameter values using non-linear least squares; CONTIN [30, 31] considers the

spectrum of the PALS as a convolution of the resolution function and Laplace transform function, while the continuous spectrum of the PALS is obtained through the inverse Laplace transform; the MELT program [31, 32] also allows one to obtain a continuous distribution of positron time, analyzing the spectrum of the PALS based on the maximum entropy principle. Unlike other spectrum analysis programs, the program MELT has the following advantages: 1) application of the program for filtering Poisson noise and application of the filtered solution as the initial solution of MELT allows obtaining a more stable result; 2) there is no requirement to measure the reference spectrum, and a low number of counts (generally 1 million counts) makes it possible to get a stable solution.

3.3. XRD analysis

X-ray diffraction studies were performed with CuKα radiation (1.5410Å wavelength) using XRD-7000S diffractometer (Shimadzu, Kyoto, Japan) in Bragg-Brentano geometry from 30° to 80° with the scan speed of 10.0°/min, the sampling pitch of 0.0143°, the preset time of 42.972 s at 40 kV and 30 mA. The diffraction patterns were collected using OneSight (Shimadzu, Kyoto, Japan) wide-range array high speed detector with 1280 channels.

4. Results and discussion

4.1. Results of PALS analysis

In high-molecular polymers positrons not only directly annihilate with electrons, but also form a metastable state "positronium" with electrons, followed by annihilation. There are two basic states of positronium: 1) parapozitronium (p-Ps), the spins of the electron and the positron are antiparallel, the intrinsic lifetime of p-Ps in vacuum is 125 ps; 2) orthopositronium (o-Ps), the spins electron and positron are parallel, the intrinsic lifetime of in vacuum is 140 ns. Due to the fact that the positronium size is only 1.06 Å and most o-Ps are formed in free volumes with subsequent annihilation, measurement of o-Ps annihilation parameters allows obtaining information about the microstructure of high-molecular polymers, while the lifetime and intensity show the size and quantities of the free volume, respectively [33].

A high-molecular polymer is a complex system. Generally, it is considered that in a high-molecular polymer there are 2 regions: crystalline and non-crystalline. The free volumes are

distributed in the non-crystalline region. Thus, there are several mechanisms of positron annihilation in solid polymers: Pick-off annihilation of o-Ps, self-annihilation of p-Ps, annihilation of free positrons in the crystalline region, and annihilation of positrons in various capture states. Attention should be paid to the fact that in practical polymers there are many different capture states, for example, in a non-crystalline region there is a capture state with a a long lifetime component, value of which is close to lifetime of o-Ps and in the crystalline region there is possibly the capture state with a short lifetime component, value of which is close to lifetime of p-Ps. In spite of many possible types of capture states, in the practical work of analyzing the spectrum of the PALS, the model of the 3 lifetime components allows obtaining a good processed result, in this case, τ_1 – the lifetime of p-Ps and positrons annihilating in the capture states with a short lifetime, τ_2 – the lifetime of free positrons annihilating in the crystalline region, τ_3 – the lifetime of the Pick-off annihilation of o-Ps and positrons annihilating in the capture states with a long lifetime. τ_2 only depends on the crystalline part, whereas only the non-crystalline region affects τ_3. As a result, the model of the 3 lifetime components satisfies the requirement to study the change of free volumes that exist only in the non-crystalline region. Table 5 shows the lifetimes of the 3 components and their corresponding intensities [34].

According to the principle of quantum mechanics, the Tao and Eldrup scientists obtained a relation between the radius of a spherical free volume and the lifetime of o-Ps [35]:

$$\tau_3 = \tau_0 \left[1 - \frac{R}{R+\Delta R} + \frac{1}{2\pi}\sin\left(\frac{2\pi R}{R+\Delta R}\right)\right]^{-1}, \quad (9)$$

Where τ – lifetime of o-Ps in free volume;

τ_0 – The lifetime of o-Ps in the electron layer surrounding the free volume, $\tau_0 = \frac{1}{2}$ ns;

R – The radius of the spherical free volume;

ΔR – Thickness of the electron layer formed on external electrons of free volume, on which annihilation of o-Ps occurs, $\Delta R = 1.656$ Å.

Free volume is

$$V = \frac{4}{3}\pi R^3 \quad (10)$$

Table 5. The lifetimes of the 3 component and their corresponding intensities.

Absorbed dose, MGy	τ_1, ($\times 10^{-12}$s)	τ_2, ($\times 10^{-12}$s)	τ_3, ($\times 10^{-12}$s)	Free volumes, 10^{-3} nm^3
0	121	315	1292	37.90
0.13	127	318	1259	35.57
0.26	134	322	1227	33.36
0.39	126	314	1235	33.90
0.52	121	318	1229	33.49

0.65	122	321	1246	34.67
Absorbed dose, MGy	I_1, %	I_2, %	I_3, %	Crystallinity, %
0	41.2±0.7	51.3±0.7	5.7 ± 0.1	90
0.13	41.3±0.7	51.1±0.6	5.8±0.1	89.81
0.26	43.2±0.9	49.5±0.9	5.6±0.1	89.84
0.39	42.5±0.8	50.8±0.7	5.1±0.1	90.88
0.52	42.6±0.7	50.4±0.6	5.4±0.1	90.32
0.65	42.0±0.7	50.7±0.6	5.7 ± 0.1	89.89

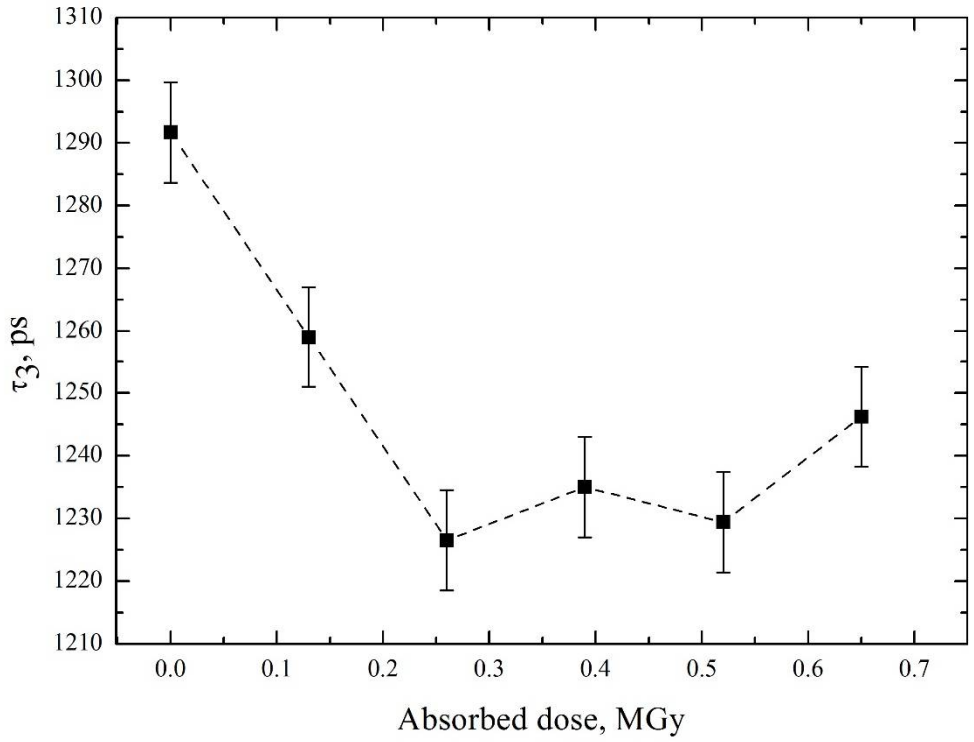

Fig.3. Dependence of τ_3 on absorbed dose.

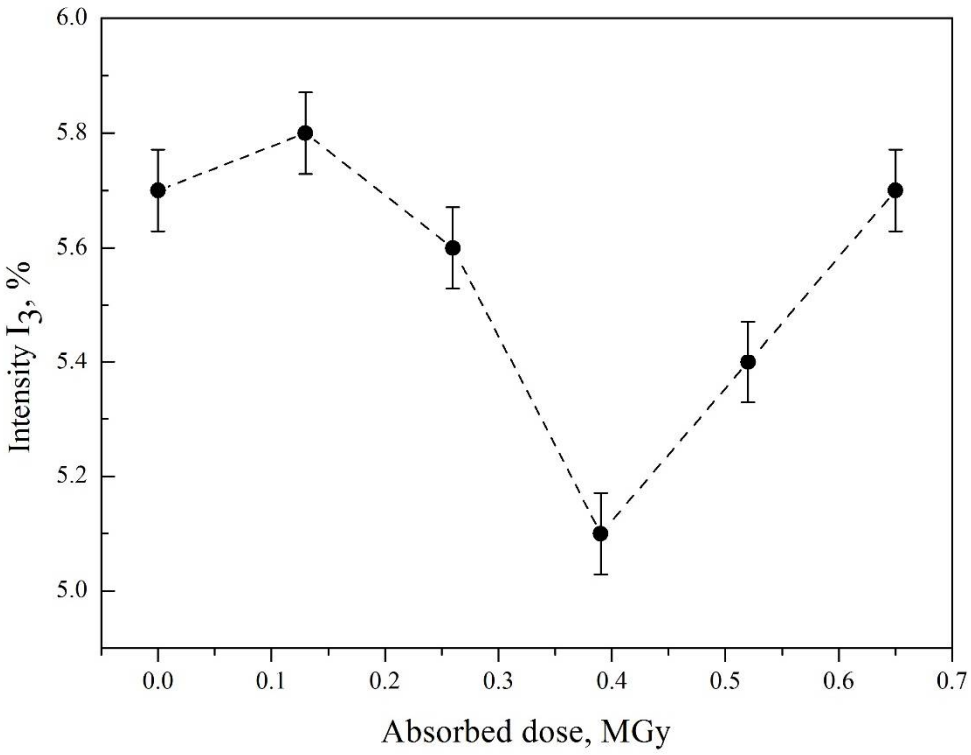

Fig.4. Dependence of intensity I_3 on absorbed dose.

It can be seen from Fig. 4 that I_3 does not change with absorbed dose below 0.25 MGy, since PVDF has a high radiation resistance. In the range 0.25 ~ 0.4 MGy, the intensity I_3 decreases, whereas with further increase in the absorbed dose, the intensity I_3 increases, this is explained by the fact that at a low absorbed dose the main process that occurs when α particles interact with high-molecular chains of PVDF is the cross-linking of chains, with a further increase in the absorbed dose, degradation of chains predominates over cross-linking of chains, which leads to an increase in the non-crystalline region. It is known that the energy of the C-C bond is 332 kJ /mol^{-1}, the energy of C-H bond is 414 kJ /mol^{-1}, the energy of C-F bond is 489 kJ /mol^{-1}. As a result, it is believed that the cross-linking and degradation of the molecular chains of PVDF is mainly carried out by the formation and decomposition of the C-C bonds.

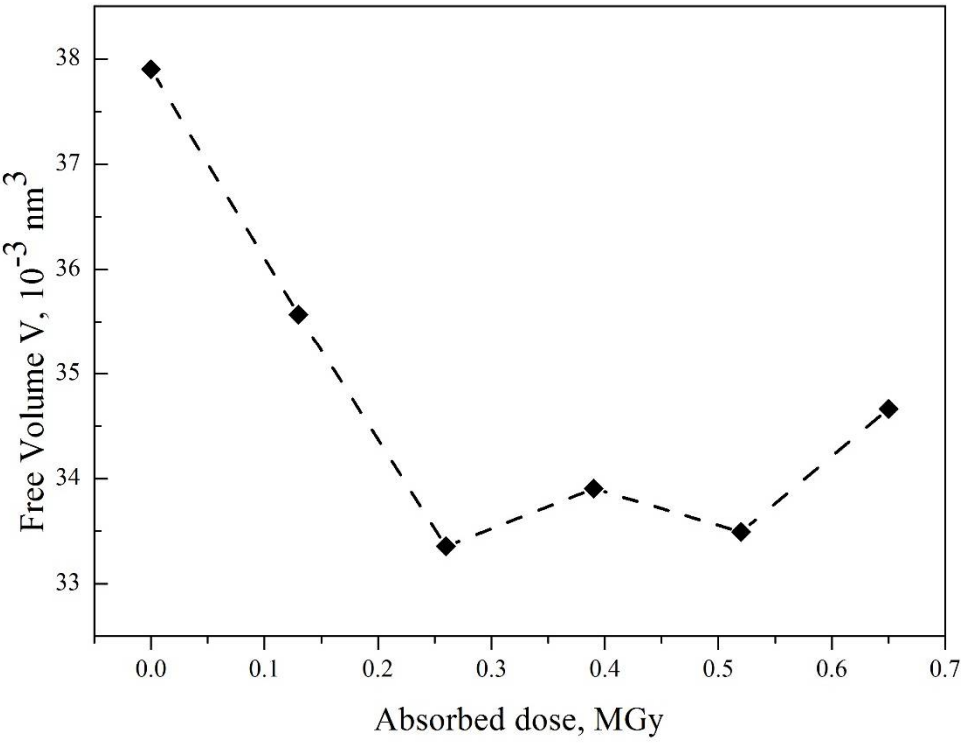

Fig.5. Dependence of free volumes on absorbed dose.

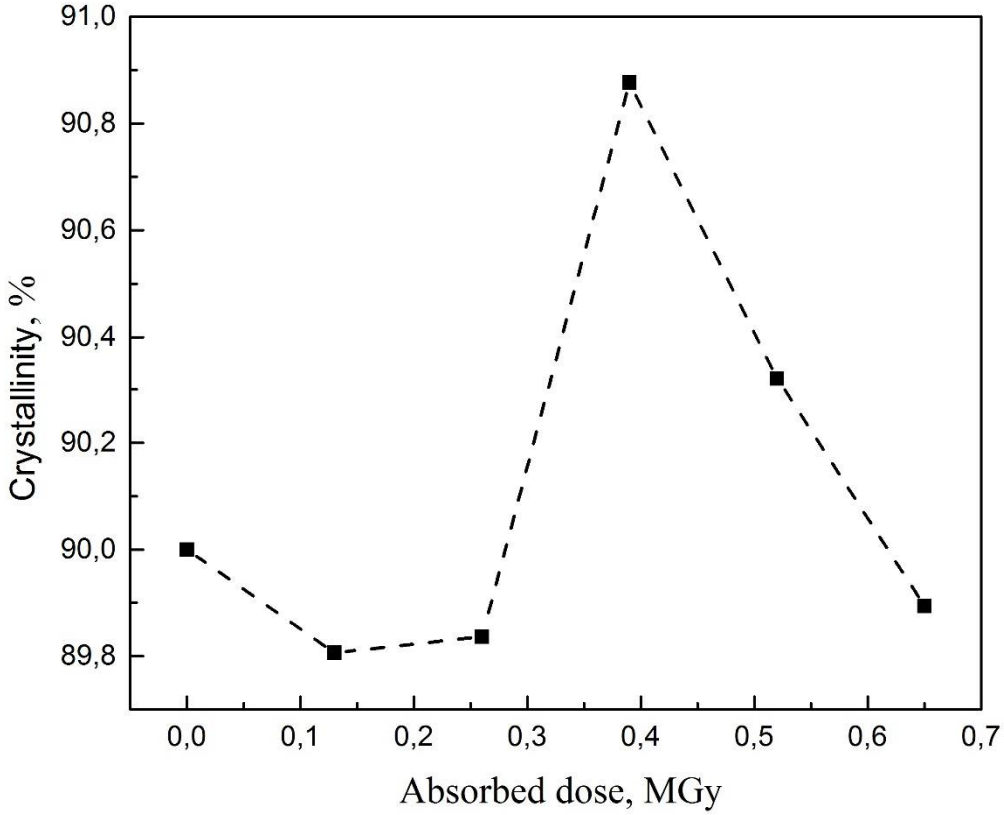

Fig.6. The crystallinity from the absorbed dose, determined by the ratio $I_2/(I_2 + I_3)$.

It can be seen from Figures 5 and 6 that at an absorbed dose below 0.25 MGy, the free volume decreases rapidly, it is noted that in this range of absorbed dose the crystallinity does not change. This behavior is explained by the characteristics of the cross-linking and degradation processes of the molecular chains of PVDF, which are presented in Fig. 7. At a low dose, segments of molecular chains in the non-crystalline region begin to move and are prepared for cross-linking with each other (processes (a), (b)). In this process, a redistribution of space occupied by free volumes and segments of molecular chains occurs in such a way that several segments enter the free volume and leave in their place a new free volume. As a result, the proportion of non-crystalline region is not changed, but the size of the free volume decreases. In the range 0.25 ~ 0.4 MGy, the discrete previous segments of the molecular chains, having entered in the free volumes, begin to cross-link and transform into ordered long molecular chains, which leads to the growth of the crystal region with an unchanged size of free volumes in PVDF (process (c)). In the range 0.4 ~ 0.65 MGy occurs the reverse process of process (c) (process (d)). It should be noted that not only new cross-linked molecular chains are degraded, but also inherent ("old") long molecular

chains in the crystalline region, it is for this reason that an increase in the non-crystalline region and in the size of free volumes is observed at a high absorbed dose.

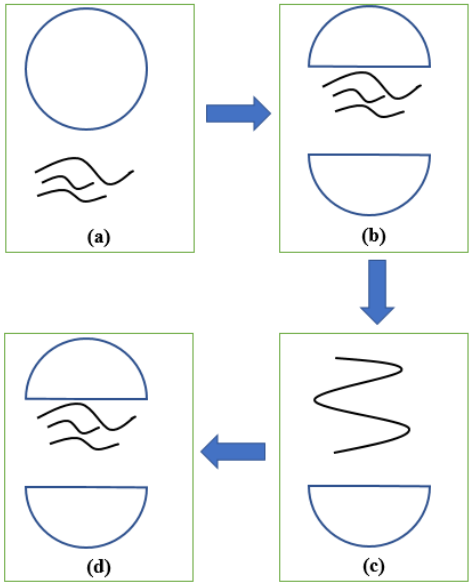

Fig.7. Process of cross-linking and degradation of molecular chains of PVDF under irradiation of helium ions.

4.2. Results of XRD analysis

XRD analysis is a technology for analyzing the structure of substances based on the diffraction effects of x-rays in crystalline materials. Each condensed material has a certain crystalline structure, including the type of lattice, the distance between the crystalline planes, and etc. When the crystalline plane of a substance is irradiated by X ray with sufficient energy, backscattering takes place, which obeys the Bragg's law.

$$2d\sin\theta = n\lambda, \quad (11)$$

Where

d – Distance between crystal planes;

θ – Diffraction angle;

λ – The wavelength of the X ray.

It is known that d in the non-crystalline region is greater than d in the crystalline region. This is because the crystal region is a group of ordered folded high-molecular chains, whereas in the non-crystalline region the segments of long chains are randomly distributed and the directions of the chains are different. From Bragg's law it follows that the more value of θ is, the smaller value of d and the larger crystallinity.

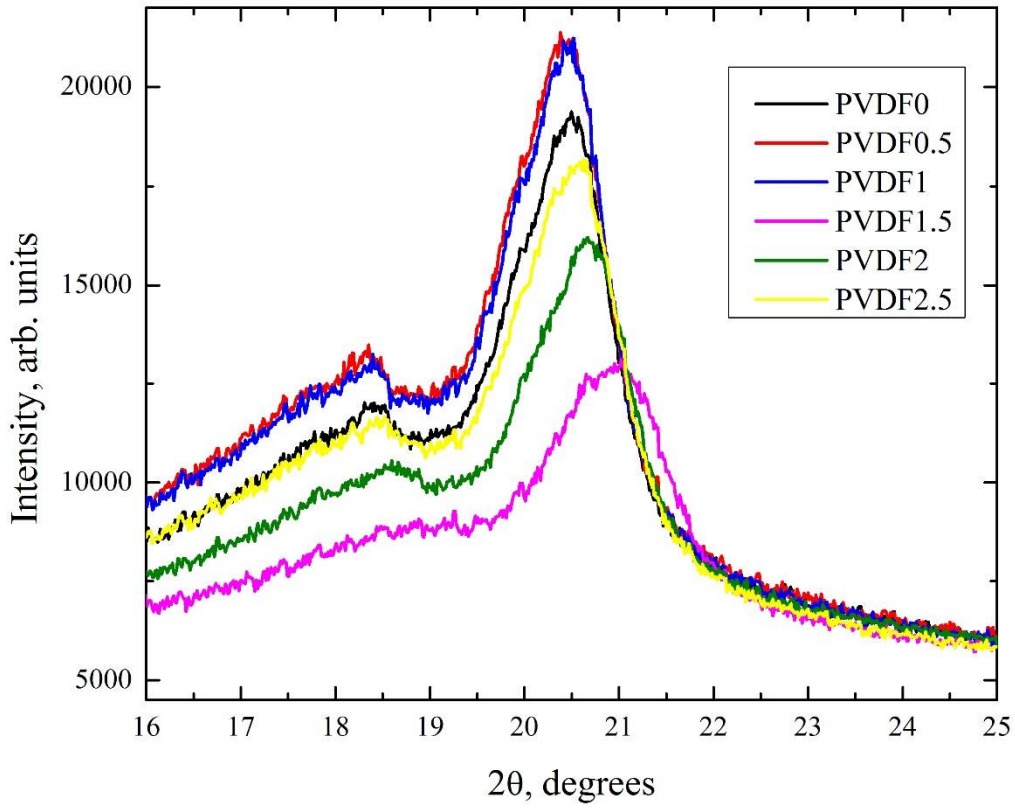

Fig.8. XRD spectrum of PVDF samples.

The XRD spectrum of PVDF samples irradiated with different doses is shown, the result is shown in Fig. 8. It is found that the largest strong peak is about 20°, which is a characteristic peak of the crystalline phase. This means that in the PVDF the main part is occupied by the crystalline phase, and also explains the low intensity of τ_3 obtained by the PALS method. Based on the XRD spectrum, the dependence of the diffraction angles on the absorbed dose was obtained (Fig. 9).

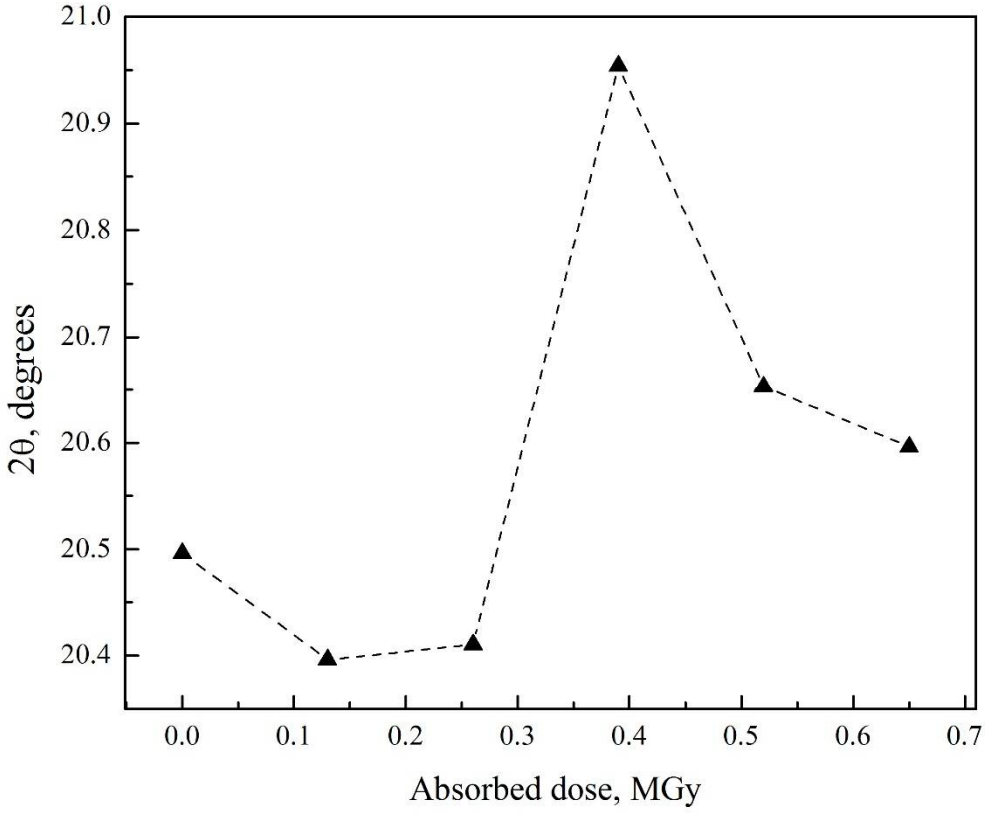

Fig.9. Dependence of 2θ on the absorbed dose.

Taking into account the proportional relationship of the crystallinity and 2θ, from Fig. 9 it follows that at a low absorbed dose (<0.25 MGy) the crystallinity does not change, at the absorbed dose in the range 0.25 ~ 0.4 MGy the crystallinity increases. With subsequent increase in the absorbed dose, the crystallinity decreases. This result coincides with the dependence of the crystallinity of PVDF on the absorbed dose obtained by the PALS method (Fig. 6)

5. Summary

Analyzing the test results measured by different methods it can be drawn that PVDF has a high resistance to radiation, and after PVDF is irradiated by Helium ions, cross-linking and degradation take place at the same time. Under different doses, the reaction mechanism is different. At an absorbed dose less than 0.25 MGy, a decrease in the free volume is observed, the crystallinity is practically unchanged. In the absorbed dose range 0.25 ~ 0.4 MGy, an increase in the crystallinity and no significant change in the free volume are observed. With a further increase in

absorbed dose, a continuous decrease in the crystallinity is observed, when the dose is raised to 0.5 MGy there is no significant change in the free volume, and a further increase in the dose to 0.6 MGy leads to its insignificant growth. This is due to the movement and cross-linking of segments of molecular chains in the non-crystalline region at a low absorbed dose and the degradation of long molecular chains at a high absorbed dose. Therefore, it is determined that the absorbed dose 0.6 MGy has exceeded the maximum damage dose of the PVDF material, at which degradation of the intrinsic crystal region of the polymer begins to occur. The results of XRD analysis confirmed the results obtained by PALS method. Interpretation and analysis of data are based on the theory of cross-linking or degradation of molecular chains (formation or decomposition of C-C bonds) PVDF.

Funding

The research is carried out within the framework of the grant of the Program for Enhancing Competitiveness of Tomsk Polytechnic University

Acknowledgments

The authors are grateful to senior researcher of the laboratory of isotopic analysis and technology TPU Sohoreva V.V. for irradiating samples.

References

[1] B. Wu, C. Wang, Y. Liu, et al. POSITRON ANNIHILATION STUDY ON THE γ-RADIATION EFFECT OF HIGH IMPACT POLYSTYRENE, J. Wuhan University Journal. 41(3) 329–332.

[2] Z.Y. Jiang, W.Z. Yu, Y.F. Zhao, et al. Influence of irradiation dose on free volume and microstructure of SIB biblock copolymer study by PALS and FT-IR, J. Acta Physica Sinica. 55(7) 3743–3747.

[3] B. Wang, ADVANCES IN THE STUDY OF POLYMERS BY POSITRON SPECTROSCOPY, J. Physics. 29(4) 196–201.

[4] W. Huang, J. Han, X.U. Yun-Shu, et al. Study on Radiation Effect of Polytetrofluoroethylene Sealing Material Irradiated by Electron Beam, J. Nuclear Physics Review. 23(2) 180–184.

[5] X. Sun, M. Zeng, G. Bao, et al. Application of positron annihilation technique for thin polymer membranes, J. Membrane Science & Technology. 26(6) 77–80.

[6] B. Wang, S. Li, C. Wang. Applications of Positron Annihilation Technique in Studying of Polymer Material Science, J. Nuclear Physics Review. 10(1) 34–38.

[7] Xia Liao, Qiongwen Zhang, Ting He, et al. Recent Advances in Application of Positron Annihilation Lifetime Spectroscopy for Polymer Microstructure Analysis, J. POLYMER MA TERIALS SCIENCE AND ENGINEERING. 30(2) 198–203.

[8] Q. Deng, K. Z. Zhang, X. J. Wang, Positron annihilation lifetime used in polymer, J. Thermosetting Resin, 2005.

[9] M.S.A.E. Keriem, Effect of Low Gamma-Irradiated dose on the Structure of Cellulose Triacetate Films: II. Positron Annihilation Spectroscopy, J. American Journal of Polymer Science, 5(2) 35–40.

[10] H. Kamal, G. Sabry, SalahLotfy, et al. Controlling of Degradation Effects in Radiation Processing of Starch, J. Journal of Macromolecular Science: Part A – Chemistry. 44(8) 865–875.

[11] Y. Ito, Y. Kobayashi, Proceedings of the 6th International Workshop on Positron and Positronium Chemistry (PPC-6) - 7-11 June 1999 Tsukuba, Japan – Preface, J. Radiation Physics & Chemistry. 58(5-6) 401-401.

[12] X. Zhou, L. Zhai, D.U. Jiangfeng, et al. Free Volume Changes in γ-Irradiated Polyethylene andPolytetraflourethylene, J. Journal of Materials Science & Technology, 16(3) 302-304.

[13] K.S. Jassim, A.A. Abdullah, A.A. Al-Bayati. Free Volume Properties of Beta-Irradiated High-Density Polyethylene (HDPE) Studied by Positron Method, J. American Journal of Scientific Research, 52(52):33–41.

[14] S.J. Wang, et al., Applied positron spectroscopy, Hubei Science and Technology Press, Wuhan, 2008. (in Chinese)

[15] Jia-Han. ZHANG, Gui-Bao. GUO, Sheng-Li. AN, et.al. Synthesis and Properties of Proton Exchange Membranesvia Single-Step Grafting PSBMA onto PVDF Modified by TMAH, J. Acta Phys. -Chim. Sin.31(10) 1905–1913

[16] A. Dyussembekova, V. Sokhoreva, Polymer Membranes for Hydrogen Fuel Cells, J. Key Engineering Materials. 743 297-302.

[17] V. Sokhoreva, et al., Radiation-Chemical Modification of PVDF Films as a Method of Creating Proton-Conducting Membranes, J. Key Engineering Materials. 683 193–198

[18] RYAN O'HAYRE, SUK-WON CHA, WHITNEY G. COLELLA, FRITZ B. PRINZ, Fuel Cell Fundamentals, 3nd ed., Publishing House of Electronics Industry, Beijing, 2007, pp. 19–143. (in Chinese)

[19] Colleen S. PEM Fuel Cell Modeling and Simulation Using MATLAB, Publishing House of Electronics Industry, Beijing, 2013, pp. 12–94. (in Chinese)

[20] Yi, B. L, Fuel Cell – Principles, Technology, Apply, Chemical Industry Press, Beijing, 2003, pp. 9–13. (in Chinese)

[21] J. Dryzek, K. Siemek, The detection of reverse accumulation effect in the positron annihilation profile of stack of aluminum and silver foils, Nukleonika. 60 (2015) 713–716.

[22] K. Siemek, J. Dryzek, The Computer Code for Calculations of the Positron Distribution in a Layered Stack Systems, 125 (2014).

[23] Jerzy Dryzek, Dong Singleton. Implantation profile and linear absorption coefficients for positrons injected in solids from radioactive sources ^{22}Na, and ^{68}Gen\$^{68}$Ga, J. Nuclear Instruments and Methods in Physics Research. B 252(2006) 197–204

[24] J. Dryzek, E. Dryzek. Measurement of backscattering coefficient of positron using the characteristic X-rays, J. Physics Letters. A 320(2003) 238–241

[25] V.I. Bespalov, Interaction of ionizing radiation with substance, 5nd ed., Publishing house of Tomsk Polytechnic University, Томск, 2014.

[26] E.M. Solov ’ev, B. V Spitsyn, R.S. Laptev, A.M. Lider, Y.S. Bordulev, A.A. Mikhailov, Analysis of the Vacancy System of Restructured Zinc by the Positron Annihilation Method, Technical Physics. 63 (2018) 834–837.

[27] Y.S. Bordulev, K. Lee, S.R. Laptev, N.V. Kudiiarov, M.A. Lider, Positron spectroscopy of defects in hydrogen-saturated Zirconium, 2016.

[28] P. Kirkegaard, N.J. Pedersen, and M. Eldrup, PATFIT-88: A Data-Processing System for positron Annihilation Spectra on Mainfraime and personal Computers. RisΦ Nalional Laboratory, Demark. 1989.

[29] J. Kansy, Microcomputer program for analysis of positron annihilation lifetime spectra, J. Nuclear Instruments & Methods in Physics Research. 374(2) 235–244.

[30] W.Z. Yu, W. Sun, The positron annihilation lifetime spectrum calculated using the CONTIN(PALS2) program, J. Nuclear technology. 23(6) 411–417. (in Chinese)

[31] G. Dlubek, S. Eichler, Do MELT or CONTIN Programs Accurately Reveal the o-Ps Lifetime Distribution in Polymers? Analysis of Simulated Lifetime Spectra, J. Physica Status Solidi. 168(2) 333–350.

[32] A. Shukla, M. Peter, L. Hoffmann, Analysis of positron lifetime spectra using quantified maximum entropy and a general linear filter, J. Nuclear Instrument &. Methods A. 335(1-2): 310–317.

[33] Y.C. Jean, Positron Annihilation Spectroscopy for Chemical Analysis: A Novel Probe for Microstructural Analysis of Polymers, J. Microchemical. 42 72–102

[34] G.H. W, Physics of Particle Interaction with Solids, Science Press, Beijing, 1991. (in Chinese)

[35] S.J. Wang, et al., Applied positron spectroscopy, Hubei Science and Technology Press, Wuhan, 2008. (in Chinese)